THE ROYAL SOCIETY

Published online 1 May 2002

Cluster size distributions: signatures of self-organization in spatial ecologies

Mercedes Pascual[1*], Manojit Roy[1], Frédéric Guichard[2] and Glenn Flierl[3]

[1]*Department of Ecology and Evolutionary Biology, University of Michigan, Ann Arbor, MI 48109-1048, USA*
[2]*Department of Ecology and Evolutionary Biology, Princeton University, Eno Hall, Princeton, NJ 08544, USA*
[3]*Department of Earth, Atmospheric and Planetary Sciences, Massachusetts Institute of Technology, Cambridge, MA 02139, USA*

Three different lattice-based models for antagonistic ecological interactions, both nonlinear and stochastic, exhibit similar power-law scalings in the geometry of clusters. Specifically, cluster size distributions and perimeter–area curves follow power-law scalings. In the coexistence regime, these patterns are robust: their exponents, and therefore the associated Korcak exponent characterizing patchiness, depend only weakly on the parameters of the systems. These distributions, in particular the values of their exponents, are close to those reported in the literature for systems associated with self-organized criticality (SOC) such as forest-fire models; however, the typical assumptions of SOC need not apply. Our results demonstrate that power-law scalings in cluster size distributions are not restricted to systems for antagonistic interactions in which a clear separation of time-scales holds. The patterns are characteristic of processes of growth and inhibition in space, such as those in predator–prey and disturbance–recovery dynamics. Inversions of these patterns, that is, scalings with a positive slope as described for plankton distributions, would therefore require spatial forcing by environmental variability.

Keywords: lattice-based models; self-organization; power-law scalings; local antagonistic interactions

1. INTRODUCTION

The 'colour' of population fluctuations has been a pervasive subject in the recent ecological literature, with titles such as 'From out of the blue' (Sugihara 1995), 'In the red zone' (Blarer & Doebeli 1996), and 'Red, blue, green: dyeing population dynamics' (Kaitala *et al.* 1997*a*). Although the subject has been approached with modern tools and ideas, including chaotic dynamics and stochasticity, it has deep roots in the early debate of whether population and community patterns are intrinsic, generated by ecological interactions and density dependence, or extrinsic, merely reflecting chance and environmental fluctuations (Gleason 1926; Clements 1936; Nicholson 1958; Smith 1961).

Colour in temporal dynamics results from patterns of autocorrelation and refers to the relative dominance of low and high frequencies. It has been explored with a variety of models to address population persistence, responses to environmental variability, and the existence of patterns that characterize intrinsic versus extrinsic processes (e.g. Kaitala *et al.* 1997*b*; Miramontes & Rohani 1998; Morales 1999; Petchey 2000). Clean signatures identifying these types of process have been evasive and patterns in nature most often reflect their complex interplay. The search for such signatures has, however, greatly increased our understanding of this interplay for different types of environmental fluctuations, and established reference patterns to gauge specific models. In particular, the initial observation by Cohen (1995) that complex dynamics in a variety of simple population models generated similar patterns of temporal correlation, and that these were opposite to the ones typically observed in nature, provided a stimulating starting point to address how modifications of the models altered the patterns.

In a similar vein, one can ask whether spatial models with intrinsic interactions that are local generate characteristic signatures. It is well known that spatial ecological models can generate elaborate spatial patterns in the absence of an environmental blueprint (e.g. Hassell *et al.* (1991) and numerous chapters in Dieckmann *et al.* (2000)). Are there common properties of spatial patterns that are robust to the details and parameters of the local interactions? We address this question for one class of systems in which the local interactions are antagonistic, such as those in predator–prey and host–parasite, but also disturbance–recovery, dynamics. These interactions are capable of generating oscillations, either decaying or persistent, in temporal models that ignore space and assume that individuals or patches are well mixed. When space is introduced, clusters continuously form and disappear (e.g. Rand & Wilson 1995; Pascual & Levin 1999). To search for commonalities in ecological patterns generated by local antagonistic interactions, we chose three models that incorporate both stochasticity and nonlinearity and treat individuals or the state of a site as discrete. In all three models, the local rules modifying the state of a site are simple but capture essential aspects of the processes of local growth and inhibition, present in predator–prey and

* Author for correspondence (pascual@umich.edu).

One contribution of 11 to a special Theme Issue 'The biosphere as a complex adaptive system'.

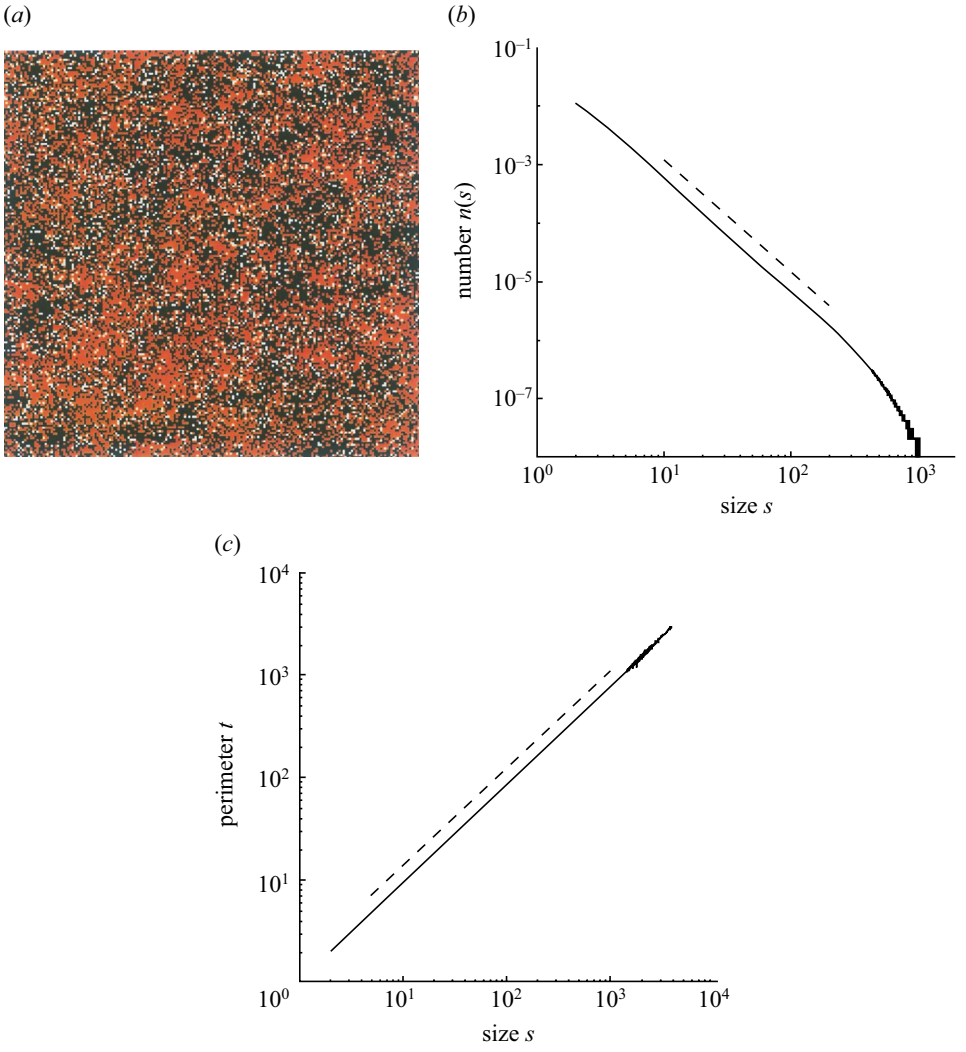

Figure 1. Spatial patterns in the predator–prey individual-based model. In the simulation, the size of the lattice is 1000×1000 and the boundaries are periodic ($\beta_1 = 1/3$, $\beta_2 = 1/10$, $\delta = 1/3$ and $\nu = 1$). (*a*) Clusters are shown for a snapshot of the lattice and for 200×200 sites after transients have died out. Prey sites are red, predator sites are white, and empty sites are black. (*b*) The cluster size distribution shown for the prey in a log–log plot. Cluster frequency decays as a power law with size. The dotted line indicates the fitted line with slope -1.99. (*c*) The perimeter $t(s)$ plotted as a function of cluster size. The dotted line shows the fitted line with a slope of 0.97 and an intercept of 0.974. For both (*b*) and (*c*), all prey clusters in 5000 time-steps were considered.

disturbance–recovery dynamics. We show that the three models exhibit remarkably similar properties in the geometry of patches or clusters. In particular, the size distribution of clusters exhibits power-law scaling with many small clusters and progressively rarer large ones. Not only is the type of distribution similar but the associated exponent is similar among the different models. This exponent depends only weakly on the specific parameter values of the models and is indicative of a high degree of patchiness. It is indeed related to the so-called Korcak exponent previously applied in ecology to characterize patchiness (Hastings *et al.* 1982; Hastings & Sugihara 1993). Another striking power law characterizes the geometry of the clusters and appears robust across the different models. The perimeter of the clusters scales as a power law with their size, and does so at almost the highest possible rate, with the exponent close to unity. From this scaling, it can be shown that the ratio of perimeter to interior becomes independent of cluster size, and that all clusters have an extensive boundary.

Robust scale invariance in cluster-size distributions has been observed in other models and in related data for disturbance–recovery dynamics (Drossel & Schwabl 1992; Solé & Manrubia 1995; Malamud *et al.* 1998; Alonso & Solé 2000). In particular, power-law scalings with similar exponents have been described for FFMs in association with SOC. We briefly discuss these models to show the generality of the patterns described here. FFMs differ, however, from our predator–prey systems in their underlying assumptions of openness and separation of time-scales. Thus, taken together, the models described here and those in the literature show that power-law scalings in cluster-size distributions and their specific exponents are generic properties of spatial systems whose intrinsic local processes involve antagonistic interactions. We therefore argue that strong deviations from these patterns, such as those previously observed in phytoplankton distributions, must necessarily involve spatial variability of the environment.

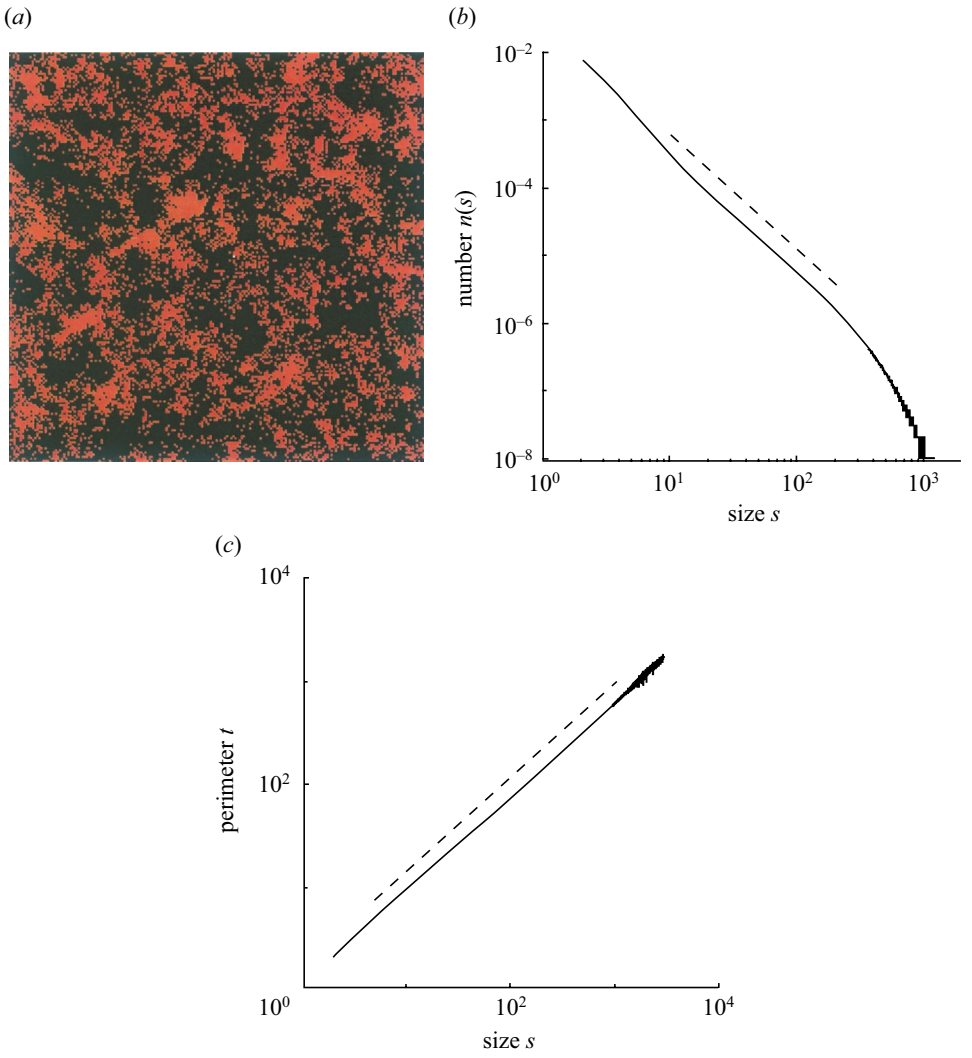

Figure 2. Spatial patterns for the prey in the food-web model. (*a*) Sites with prey are coded in red and those with no prey are coded in black. (*b*) The cluster size distribution for the prey decays as a power law with an exponent of -1.75. (*c*) The perimeter scales as a power law with cluster size, and with an exponent of 0.92. For further details see figure 1 caption.

2. INDIVIDUAL-BASED PREDATOR–PREY DYNAMICS

The first predator–prey model is an interacting-particle system (Durrett & Levin 2000) and a successor of an earlier cellular automaton which incorporated individual age (Dewdney 1988; Sutherland & Jacobs 1994 (we return to this more detailed version later in § 7)). Space in the model is given by a 2D lattice in which each site is either occupied by a prey, occupied by a predator, or empty. All processes are local and depend on the state of neighbouring sites.

The particular neighbourhood we consider in the simulations consists of the four nearest sites. Prey growth occurs as a contact process: a prey chooses a neighbouring site at random and gives birth onto it only if this site is empty at rate β_1. Predators hunt for prey by inspecting their neighbourhood for the presence of prey at rate 1. If prey are present, the predator selects one at random and eats it, moving to this neighbouring site. Only predators that find a prey can reproduce, and do so with a specified probability, β_2. The offspring is placed in the original site of the predator. Predators that do not find prey are susceptible to starvation and die with a probability δ. Random movement occurs through mixing: neighbouring sites exchange state at a constant rate ν. Stochasticity in the model is demographic: the above rates specify probabilities for the associated events to happen in a given interval of time. Specifically, an event occurs at times of a Poisson process with the specified rate. The model is also nonlinear as the rates of local growth and predation depend on local densities.

Simulations have shown that after transients die out, prey clusters continuously change as they form and disappear through prey growth and predation (Pascual & Levin 1999; Durrett & Levin 2000). Similar clustering is produced by other predator–prey systems on 2D lattices (e.g. Rand & Wilson 1995). Typical patterns are illustrated with a snapshot of the lattice for one particular parameter set (figure 1*a*). Prey clusters appear to span a wide range of sizes, with spatial correlations developing well beyond the size of the local neighbourhood of interaction.

To characterize these patterns, we define a prey cluster as a group of prey sites connected to each other by neighbourhood distances, where the neighbourhood of a site is identical to that used in the model. We consider the number $n(s)$ of clusters with a given area s, normalized by the total number of clusters on the grid, where the size or area

Table 1. Values of exponent α for prey clusters in the individual-based predator–prey model as a function of parameters β_2 (first row) and δ (first column).
(In all simulations, transients are removed for 5000 time-steps. The exponent is computed from the size distribution obtained for the following 2000 time-steps, and estimated by linear least-square regression. The s.d. are given in parentheses. The exponent is close to 2 and shows the largest deviations from this value when the probability of reproducing is high and that of starving is low for the predators.)

δ/β_2	0.15	0.30	0.45	0.60	0.75	0.90
0.15	2.3730 (0.0032)	2.4902 (0.0046)	2.5923 (0.0061)	2.7310 (0.0083)	2.8731 (0.0110)	2.9442 (0.0132)
0.30	2.1027 (0.0030)	2.2687 (0.0051)	2.2966 (0.0065)	2.3497 (0.0064)	2.4446 (0.0060)	2.5375 (0.0058)
0.45	1.9736 (0.0040)	2.1730 (0.0054)	2.2049 (0.0074)	2.2218 (0.0080)	2.2626 (0.0074)	2.3229 (0.0068)
0.60	1.9116 (0.0052)	2.1099 (0.0054)	2.1601 (0.0075)	2.1675 (0.0090)	2.1864 (0.0087)	2.2162 (0.0083)
0.75	1.8842 (0.0057)	2.0618 (0.0054)	2.1327 (0.0073)	2.1434 (0.0085)	2.1484 (0.0089)	2.1611 (0.0090)
0.90	1.8757 (0.0063)	2.0286 (0.0050)	2.1063 (0.0072)	2.1248 (0.0086)	2.1292 (0.0091)	2.1375 (0.0094)

s is given by the number of sites in the cluster. Figure 1*b* shows the distribution of prey clusters on a log–log scale for $n(s)$ as a function of s. The distribution exhibits power-law decay over two orders of magnitude with

$$n(s) \propto s^{-\alpha}, \tag{2.1}$$

and exponent $\alpha = 1.99$ (s.d. = 0.0048). Such power-law distributions have been previously applied to describe ecological patchiness but in their cumulative form (Hastings & Sugihara 1993). In this form, the number of clusters $N(S)$ with a size larger than a given value a is given by

$$N(s) \propto s^{-B}, \tag{2.2}$$

where the exponent B is known as the Korcak exponent. A cumulative distribution of this form was first introduced by Korcak to describe the size distribution of Aegean islands (Korcak 1938; see Hastings & Sugihara (1993) for ecological discussion). Clearly, the exponents α and B are related to each other with $B = \alpha - 1$. The value $B = 0.99$ obtained here for prey clusters is indicative of a high degree of patchiness, that is of patterns with many small patches and a long tail in the size distribution.

Although the results presented so far apply to one particular parameter set, they are representative of parameter space as a whole. In particular, the existence of a power-law scaling for the cluster-size distributions is independent of the values of β_2 and δ in the coexistence regime. Only the size range over which the scaling holds varies, as the maximum cluster size in the system also varies. More importantly, however, the values of the exponents (α and B) characterizing the size distributions depend only weakly on parameter values. This is illustrated in table 1 for the probabilities β_2 and δ. A similar range of exponents was observed for different values of β_1 (results not reported here).

Another striking geometrical property regards the relationship between the perimeter and the area of prey clusters. It is at this boundary that the processes of prey growth and predation occur. Therefore, its extent effectively determines how space alters the rates of these processes. We describe here another power-law scaling which demonstrates a fast accumulation of perimeter with area, and implies a low interior fraction for the clusters, regardless of their size.

We define the perimeter of a prey cluster as the set of prey sites belonging to the cluster with at least one non-prey neighbour (where a non-prey site is either occupied by a predator or empty). The mean perimeter $t(s)$ is then given by averaging over the size of individual perimeters for all clusters of the same area s. Figure 1*c* shows that the perimeter scales with the area as

$$t = bs^{\gamma}, \tag{2.3}$$

with the exponent γ very close to unity. Thus, the perimeter grows as a power law of the area and does so almost at the fastest possible rate. Compare this observation with that expected for clusters with a regular geometry for which the perimeter scales as $s^{0.5}$.

Figure 1*c* also shows that the scaling coefficient b is itself close to unity, as the intercept of the line is close to the origin of the log–log plot. The twin results γ, $b \approx 1$ are important indicators of the ramified structure of prey clusters. This can be illustrated by defining the cluster interior fraction $f(s) = (s - t)/s$ and noting that

$$f(s) = 1 - bs^{\gamma - 1}. \tag{2.4}$$

For $\gamma \approx 1$, it follows that $f \approx 1 - b$ and therefore that the interior fraction f becomes almost independent of cluster size. Furthermore, for $b \approx 1$, the value of f is close to zero and the clusters have very small interior, irrespective of their sizes. This observation is easily confirmed by directly computing f as a function of s. Not only does it remain constant but, for the simulation of figure 1, it does so at a value of 0.20. In other words, on average, almost 80% of the cluster area is made up of its perimeter. These results are again robust to changes in parameter values: the exponent γ depends only weakly on the rates of predation and growth. For example, for the values of β_2 and δ_2 in table 1, γ falls in the interval (0.92, 0.96).

Thus, the local interaction of predator and prey generates patterns with characteristic power-law scalings in the cluster-size distribution and in the perimeter–area relationship. We show next that the same power-law scalings are produced by another predator–prey system, in which the resource that limits prey growth is modelled explicitly.

3. INDIVIDUAL-BASED FOOD-WEB DYNAMICS

The second model is motivated by predator–prey interactions in plankton. In particular, the growth of the prey is determined by a limiting nutrient, which diffuses freely to adjacent sites in the lattice. The space as before is 2D but sites within the lattice can harbour multiple individ-

Table 2. Values of exponent α for the prey clusters in the food-web model as a function of parameters β_2 (first row) and δ (first column).
(The values of this exponent are given only for the region of parameter space in which we observe coexistence and a continuous cluster size distribution. For low grazing (low β_2) and high starvation probabilities (high δ), the predator is unable to persist and the system reaches an absorbing state with the prey occupying the whole lattice. As for table 1, transients are removed for 5000 time-steps. The coexistence of predator and prey is verified for a much longer period (20 000).)

δ/β_2	0.15	0.30	0.45	0.60	0.75	0.90
0.15	—	1.8433 (0.0032)	1.8233 (0.0052)	1.8418 (0.0050)	2.0117 (0.0130)	2.1746 (0.0194)
0.30	—	—	1.8249 (0.0043)	1.8029 (0.0074)	1.7055 (0.0058)	1.6790 (0.0033)
0.45	—	—	—	1.8640 (0.0052)	1.7791 (0.0083)	1.6995 (0.0075)
0.60	—	—	—	—	1.8578 (0.0064)	1.7583 (0.0084)
0.75	—	—	—	—	2.0921 (0.0027)	1.8288 (0.0073)
0.90	—	—	—	—	—	1.9298 (0.0056)

uals for both the predator and prey. The sites can be thought of as areas over which the nutrients are accessible to prey and over which predators can forage during a time-step. The presumption is that this region is large enough to contain a number of individuals but smaller than the scale of groups. Predation and reproduction occur within a site, and the spatial coupling between sites occurs through the random mixing of individuals and the diffusion of nutrients.

We implement the model as a cellular automaton by treating time as discrete and therefore synchronously updating the sites in the lattice. In one time-step, a prey takes up nutrients within the same site with a probability β_1. For simplicity, we assume that the nutrient concentration has been normalized so that uptake occurs in units of one. Nutrient uptake by a prey leads to production of one offspring in the same site. A predator finds and eats prey with a probability β_2, in which case it produces one offspring in the same site. If the predator fails to find a prey, it starves and dies with a probability δ. So far all processes are local, applying to each individual within a site. Once the whole lattice is updated, random mixing of individuals and nutrients couples the dynamics of the system across sites. Each predator and prey moves, with a probability ν to one of the sites in a local neighbourhood given by the four nearest neighbours and the original site. The same neighbourhood is used to implement the movement of nutrients with a diffusion coefficient D, by discretizing the diffusion operator. In all simulations, boundaries are periodic.

Simulations of the model show that the prey aggregates into patches. To characterize these spatial patterns, we focus as before on the size of prey clusters. To define clusters, we first translate the spatial distribution of abundances into presence or absence of the prey population in a site. Figure 2*a* shows a snapshot of the resulting clusters. After transients die out, these clusters form and disappear continuously throughout space, as nutrients fluctuate and populations of prey and predators go locally extinct but recolonize new sites. The resulting size distribution is similar to the one described before for the individual-based predator–prey model. It is given by a power law with exponent $\alpha = 1.75$ (0.0049) (figure 2*b*). In the coexistence regime, the value of this exponent varies weakly with model parameters. This is shown in table 2 for the parameters of the predator–prey interaction.

A power-law scaling also holds for the perimeter of the clusters as a function of area (figure 2*c*). The exponent is again almost unity ($\gamma = 0.92$) and it varies weakly with the parameters of the interactions, falling within the interval (0.87, 0.99) for the parameters of table 2. The associated interior fraction is again low, with the perimeter accounting on average for 75% of the cluster in the simulation of figure 2.

Thus, the two models exhibit similar power-law scalings for the prey clusters, in spite of significant differences in the details of the processes and implementation. The food-web model is implemented as a cellular automaton, while the predator–prey model is an interacting-particle system. The former model further considers a spatial scale of interaction larger than that of the individuals, in which sites of the lattice contain subpopulations of the predator and prey. The spatial coupling across subpopulations is given through the diffusion of nutrients and the random mixing of individuals. In both models, however, the local growth of clusters is limited by a resource, either space or nutrients, and inhibited by predation. Similar processes of growth and inhibition occur in the spatio-temporal dynamics of disturbance and recovery. We consider this type of dynamics next; first with a model for gap dynamics in intertidal mussel beds, and then through comparison with the literature on forest-fire dynamics.

4. DISTURBANCE–RECOVERY DYNAMICS

The MDM was developed to explore the role of local interactions between physical disturbance and biological processes in marine benthic communities (Guichard *et al.* 2002). In communities dominated by mussels, wave action is often an important source of disturbance, creating gaps in the mussel bed which are progressively recolonized by a series of opportunistic species and finally by mussels. The model is lattice based and describes space occupancy by mussels over a homogeneous midzone intertidal area.

The MDM assumes that a few strong waves create initial gaps in the mussel bed but that most waves are only able to spread the disturbance by removing unstable mussels along recently disturbed edges. Similarly, the MDM assumes that mussels will recolonize gaps along edges of the bed, thus allowing nearest-neighbour interactions for both disturbance and recovery (recolonization). MDM was built as a generalized FFM allowing local interactions

Table 3. Values of exponent α for clusters of the mussel bed in the disturbance–recovery model, as a function of parameters α_d (first row) and α_r (first column).
(In all simulations, transients are removed for 5000 time-steps. The exponent is estimated by linear least-square regression for the size distribution obtained in the following 2000 time-steps. Values are reported only for the cases in which the different types coexist and the size distribution is continuous. If the disturbance probability is not sufficiently high, the mussel bed takes over and the system reaches an absorbing state. For the reported values, we consider that the system is in the coexistence regime if all types persist after 20 000 time-steps. The size of this region depends also on the rate at which new disturbances are initiated, which has been kept constant here. The exponent shows the largest deviations from a value of 2 when both the disturbance and the recovery probability are high.)

α_r/α_d	0.80	0.85	0.90	0.95	1.00
0.550	—	—	—	—	1.9115 (0.0027)
0.625	—	—	—	1.9349 (0.0031)	1.8040 (0.0031)
0.700	—	—	2.0105 (0.0034)	1.8380 (0.0028)	1.7283 (0.0031)
0.775	—	—	1.9174 (0.0024)	1.7735 (0.0025)	1.6788 (0.0030)
0.850	—	2.0603 (0.0028)	1.8533 (0.0026)	1.7210 (0.0027)	1.6460 (0.0024)
0.925	—	1.9901 (0.0031)	1.8031 (0.0025)	1.6873 (0.0023)	1.6232 (0.0024)
1.000	—	1.9410 (0.0024)	1.7662 (0.0026)	1.6633 (0.0023)	1.6116 (0.0018)

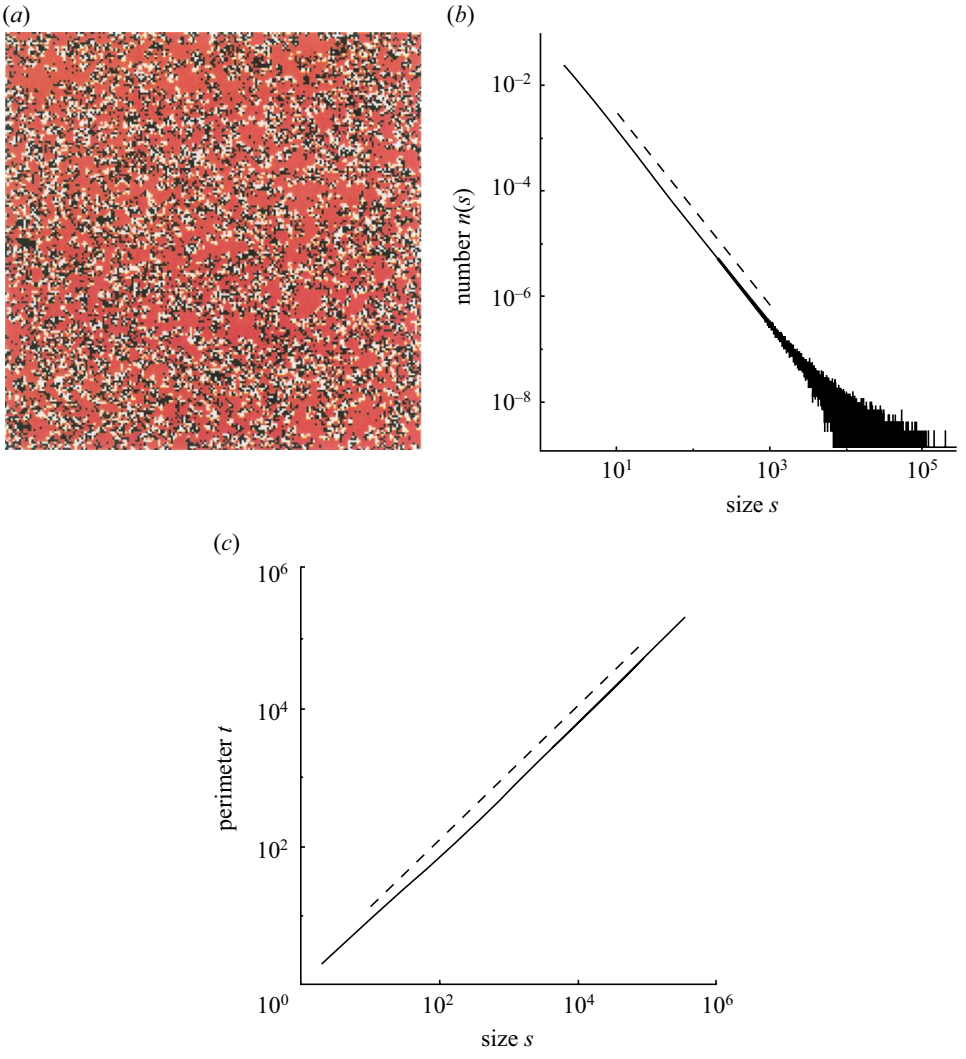

Figure 3. Spatial patterns in the mussel-disturbance model. (*a*) Red sites are occupied by the mussel bed, white sites are disturbed, and black sites are empty. (*b*) The size distribution for clusters of the mussel bed decays as a power law with an exponent of -1.82. (*c*) The perimeter scales as a power law with cluster size, and with an exponent of 0.97. For further details see figure 1 caption.

during the regrowth process, which is implemented as a constant rate in the FFM.

Each cell of the lattice is defined by three states: empty, occupied or disturbed. The disturbed state is the equivalent of burning trees in the FFM and refers to newly disturbed mussels leaving unstable edges along the bed, which is then more susceptible to disturbance. During the asynchronous update, an empty site becomes occupied with probability α_r if at least one of its four nearest neighbours is occupied. An occupied cell becomes disturbed with a probability α_d if at least one of its neighbours is disturbed. The probability of a new disturbance is $\delta_0 = 2 \times 10^{-6}$. All simulations are run with periodic boundary conditions.

The relative values of the parameters α_r and α_d determine the long-term behaviour of the system. Different asymptotic states, including absorbing ones, are possible. For example, when the disturbance probability α_d is too low relative to the probability of recovery α_r, the disturbed state is unable to persist and the mussel bed eventually covers the whole lattice. We focus here on the spatial patterns of the system when the occupied and disturbed states coexist. In this case, there is formation of clusters in the mussel bed after transients die out. Figure 3*a* shows a typical configuration of the lattice. As for the predator–prey models, the clusters continuously form and disappear at different spatial locations. The resulting cluster-size distribution decays as a power law with exponent $\alpha = 1.82$ (0.0012) (equation (2.1); figure 3*b*). This power-law scaling persists as we vary the parameters of the model within the coexistence region. The exponent itself decreases from a value close to 2 for parameters near the transition between the coexistence regime and the absorbing state, to 1.6 for high α_r and α_d (table 3).

Cluster geometry is also similar to that of the predator–prey systems with regard to the extensive nature of the boundary. Specifically, cluster perimeter grows with area as a power law with exponent $\gamma = 0.97$ (figure 3*c*). From this curve, we can again show that the interior fraction of the clusters is low with $f = 0.35$. In the coexistence regime, the exponent γ varies weakly with parameter values, falling within the interval (0.94, 0.99).

In summary, the three models described so far exhibit spatial self-organization in the coexistence regime, in the sense of generating spatial patterns characterized by power-law scalings. The patterns are characterized by the absence of a characteristic cluster size and the existence of correlations at spatial scales much larger than those at which the local processes operate. Importantly, the emergence of these patterns does not require the 'fine tuning' of any particular parameter. In fact, we have shown that not only the existence of power-law scalings but also their specific exponents are robust to changes in parameters within the coexistence region.

5. RELATED MODELS AND SOC

Similar properties have been described for other systems, specifically those associated with SOC (Bak *et al.* 1988, 1990; Drossel & Schwabl 1992). FFMs are of particular relevance here since they address dynamics for disturbance and recovery (e.g. Drossel & Schwabl 1992; Grassberger 1993). FFMs have also been applied to the dynamics of epidemics in isolated populations (Rhodes & Anderson 1996; Rhodes *et al.* 1997), with the infection propagating through small susceptible populations. Interestingly, FFMs exhibit power-law scalings in the size distribution of tree clusters, and both numerical and analytical results have demonstrated that the corresponding scaling exponent $\alpha = 2$ (Drossel & Schwabl 1992; Clar *et al.* 1999; Gabrielov *et al,* 1999). Patterns for forest fires in nature have shown remarkable agreement with predicted scalings (Malamud *et al.* 1998).

Our models differ, however, from FFMs and other SOC systems in important ways. Most importantly, they lack one key assumption of FFMs, the separation of time-scales. In FFMs associated with SOC, the sites of a lattice can be in any one of three possible states: empty, occupied by a tree, or occupied by a burning tree. Disturbances or fires propagate rapidly as trees with nearest neighbours in the burning state catch fire. New disturbances are initiated by 'lightning', which allows trees with no burning neighbours to ignite spontaneously. Recovery, the growth of trees onto empty sites, occurs via open recruitment from outside the system. Two basic parameters define key time-scales: the tree growth rate, p, and the lightning or sparking rate f. Critical behaviour and the associated power laws are found when the following condition holds:

$$t(s_{\max}) \ll p^{-1} \ll f^{-1}, \tag{5.1}$$

where $t(s_{\max})$ is the time taken by large clusters (or the order of the lattice size) to burn completely (e.g. Drossel & Schwabl 1992; Rhodes *et al.* 1997). Thus, there is a clear separation of time-scales, with defined disturbance events in which fire spreads rapidly relative to the time-scale of recovery, and long periods of stasis in which tree growth proceeds before the initiation of a new fire. This separation of time-scales is absent from our predator–prey models, and is not required in the disturbance–recovery model to produce the described power-law scalings. For the parameter range considered here, the rates of disturbance and recovery are indeed of the same order.

Another difference with FFMs is the treatment of recovery as a local process involving the state of neighbouring sites. In this regard, the predator–prey models offer an even larger contrast, as all processes are local involving nearest-neighbour interactions. The systems are in this sense closed, with no recovery (prey growth) or initiation of new disturbances (predation) driving the dynamics as an external forcing. Thus, spatial self-organization with similar patterns to those described for SOC systems is possible under a different and complementary set of assumptions.

6. TEMPORAL DYNAMICS

The lack of separation in time-scales leads also to differences in the temporal dynamics of densities between our models and systems previously associated with SOC. In the latter, time-series for the abundance or density of the disturbed state (i.e. burning fires, infected individuals) exhibit intermittent fluctuations, with short-lived bursts separated by long periods of recovery, as disturbances propagate and decay rapidly (e.g. Rhodes & Anderson 1996). The distribution of event sizes is described by a power law specifying the frequency of fires or epidemics

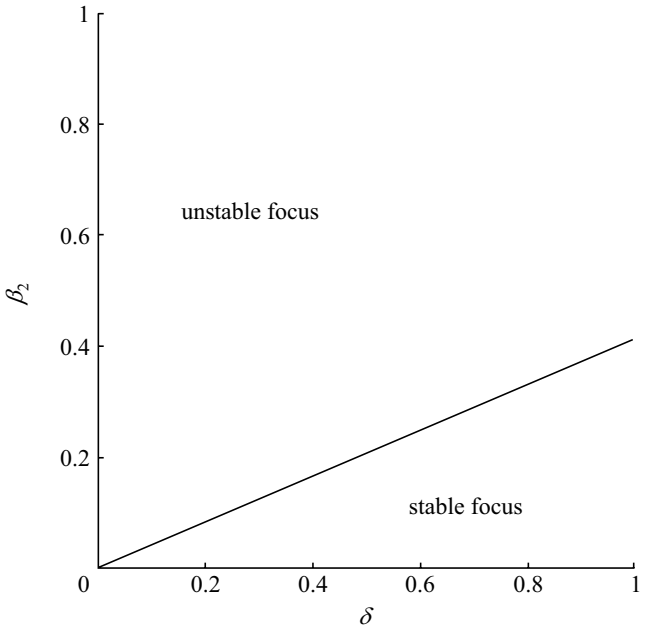

Figure 4. Parameter space β_2 (predator's probability of reproducing) and δ (predator's probability of starvation), showing the bifurcation line at which the equilibrium loses stability.

as a function of their size (e.g. Rhodes & Anderson 1996; Rhodes *et al.* 1997; see also Keitt & Marquet (1996) for an example in a different ecological context). Because disturbances propagate rapidly, event sizes in time closely reflect disturbance sizes in space.

When time-scales are comparable, as in the predator–prey and mussel-bed model, this temporal scaling does not hold. There are no intermittent short-lived events in the density of the disturbed state (i.e. predator, disturbed mussel bed) but more regular oscillations whose amplitudes decrease with the spatial scale of averaging (Rand & Wilson 1995; Pascual & Levin 1999; Durrett & Levin 2000; Pascual *et al.* 2001). These oscillations are aperiodic at intermediate scales, and become small deviations around an apparent steady state at large scales (of the size of the lattice). Pascual *et al.* (2001) provide an explanation for this change in the amplitude of the cycles and for their aperiodicity.

These temporal dynamics occur in the spatial system when the corresponding mean-field equations display either limit cycles or decaying oscillations towards an equilibrium (Durrett & Levin 2000; Pascual *et al.* 2001). The mean-field equations are written under the assumption that individuals are well mixed and that therefore, at any site in the lattice, local interactions occur according to mean densities. These equations are given in Appendix A for the predator–prey model together with the stability analysis of the equilibrium. Figure 4 shows the resulting bifurcation line separating limit cycles from an oscillatory approach to equilibrium in the parameter space (β_2, δ). Thus, oscillations, whether persistent or decaying, are always present in the mean-field dynamics for the parameters of table 1. We claim, but it remains to be shown, that this type of dynamics in the mean-field equations unifies the spatio-temporal models considered here.

7. CONCLUSIONS

We have shown that three different models, both spatial and stochastic, exhibit similar scaling patterns in the size distribution and perimeter-size relationship of clusters. These power-law scalings result from local antagonistic interactions, and imply both the lack of a characteristic cluster size and the existence of spatial correlations, at distances larger than those of the local processes, in the absence of any environmental blueprint. In this sense, we refer to the emergence of these patterns from local intrinsic interactions as spatial self-organization. The scaling exponents characterizing the patterns were also shown to depend only weakly on parameter values in the coexistence regime. The negative exponent of the size distribution reflects many small clusters accompanied by progressively rarer large clusters. From this distribution, a patchiness exponent or Korcak exponent can be computed, which in all cases is larger than 0.5 and typically close to 1, indicating a high degree of patchiness in the systems. The perimeter-size exponent is tightly clustered below 1 for all models and parameters considered. Thus, the perimeter grows rapidly with size and does so at almost the highest possible rate. Together with the intercept, the value of this exponent shows that clusters have a remarkably low interior, or equivalently an extensive perimeter, and that this feature is independent of cluster size, holding for the largest clusters.

We have varied parameters widely but away from the limit in which a clear separation of time-scales exists. Such a separation is a key assumption of FFMs, which exhibit power-law scalings in cluster-size distributions similar to the ones described here. Thus, we have argued that the existence of such power laws does not necessarily require this assumption. This scaling appears to hold for a broad class of systems for antagonistic ecological interactions, encompassing those associated with SOC and the examples in this paper. Together with the described power law for cluster perimeter, this scaling provides a signature for intrinsic dynamics in spatial systems for antagonistic interactions. We expect it to hold in other models, regardless of the details of local interactions, not only for predator–prey and disturbance–recovery but also for host–pathogen dynamics (e.g. Rand *et al.* 1995; Keeling 2000).

Evidence for power-law scalings in cluster-size distributions has been reported for vegetative ecosystems (Hastings & Sugihara 1993). The associated Korcak exponent varies across systems and with the degree of human perturbation, but values are typically larger than 0.5 and as high as 0.8 (Hastings *et al.* 1982; Hastings & Sugihara 1993; Xiao-Ping *et al.* 1999). The shapes of cluster boundaries have also attracted attention, and estimates using fractal dimensions, for example for patches in a deciduous forest, indicate a large accumulation of perimeter (Krummel *et al.* 1987; Hastings & Sugihara 1993). Further measurements of this type would be of interest.

Perhaps a more important question than whether the scalings are common in nature is under what conditions they do break down. We view these patterns as one extreme from which to examine how added realism, such as environmental heterogeneity and non-random dispersal, modifies them. An earlier study with a precursor of

WATOR in which individual age was taken into account as well as a larger neighbourhood, shows power-law scaling in the cluster-size distribution (Sutherland & Jacobs 1994). However, a break-point appears and separates two scaling regions, with a flattening of the slope for the larger clusters. A similar break appears in our model when eight instead of four adjacent neighbours are considered. Although not pronounced, it appears linked to the appearance of much larger clusters. The mechanism generating this break remains to be understood. It is interesting to note, however, that the existence of break-points in power laws has typically been interpreted as evidence for a change in the underlying processes (e.g. Bradbury *et al.* 1984; Krummel *et al.* 1987; Meltzer & Hastings 1992). No such change is present here in the predator–prey model.

A more extreme deviation from the described patterns has been observed in marine ecosystems in association with plankton. Phytoplankton patchiness has been analysed using variance spectra and typically shown to follow a power-law form but with higher variance at the larger wavelengths (e.g. Denman & Platt 1976; Gower *et al.* 1980; Weber *et al.* 1986). We can therefore infer that cluster-size distributions would exhibit a power-law scaling but with a positive slope. This inversion from the negative slope described here is consistent with the well-studied explanations for plankton patchiness and with the ingredients of models that reproduce it, including turbulent cascades and variability of the environment (e.g. Bennett & Denman 1985; Powell & Okubo 1994; Abraham 1998). We argue more generally that pronounced deviations from the patterns described here will require extrinsic factors in the form of environmental forcing.

An inverse cascade model, opposite to the one invoked for turbulence in plankton patchiness, has recently been proposed as an explanation for the dynamics and self-similar scalings of clusters in FFMs and other systems described as SOC (Gabrielov *et al.* 1999). In this cascade, elements are introduced at the smaller scale, which then coalesce to form larger and larger clusters, with the ultimate loss of the largest ones. A similar cascade from small to large clusters may arise more generally from local ecological interactions and underlie the patterns described here.

Finally, approaches to tackle the dynamics of systems with large numbers of distributed variables have been summarized as falling into two different classes: (i) those that reduce the dimensionality of the system to consider simpler and more tractable dynamical models; and (ii) those that search for simple statistical patterns characterizing the full set of variables (Keitt & Stanley 1998). Numerous examples of the former can be found in the recent literature on spatio-temporal dynamics (e.g. Levin & Pacala 1997; Dieckmann *et al.* 2000; Pascual *et al.* 2001), and of the latter, in macroecological studies. Much less understood are the links between these complementary approaches. The existence of robust power-law scalings characterizing statistical patterns may provide a basis for model simplification. A simple modification of the mean-field equations accounts for the effects of spatial pattern and approximates accurately the dynamics of population densities at large scales in one of the predator–prey systems described here (Pascual *et al.* 2001). The connection between this approach to simplify the system and the geometry of the spatial patterns remains to be explored.

M.P. acknowledges the support of the James S. McDonnell Foundation through a Centennial fellowhsip, and F.G. the support of the Andrew W. Mellon Foundation.

APPENDIX A: BIFURCATION ANALYSIS FOR THE MEAN-FIELD PREDATOR–PREY MODEL

Durrett & Levin (2000) show the existence of a Hopf bifurcation for the mean-field equations of the predator–prey model. We specifically derive here the bifurcation curve in parameter space (β_2, δ) for which the equilibrium loses stability. This curve is plotted in figure 4.

The mean-field equations for the predator–prey model are

$$\mathrm{d}p/\mathrm{d}t = \beta_1 p[1 - (p + h)] - h[1 - (1 - p)^q], \tag{A 1}$$

$$\mathrm{d}h/\mathrm{d}t = \beta_2 h[1 - (1 - p)^q] - \delta h(1 - p)^q \tag{A 2}$$

(Durrett & Levin 2000). These equations have a non-trivial equilibrium, and linearization around this point yields two eigenvalues λ_i $(i = 1,2)$ given by a conjugate pair (Durrett & Levin 2000). The real part of these eigenvalues is $\mathrm{Re}(\lambda_i) = T/2$, where T is the trace of the Jacobian matrix associated with the linear system. Thus, $\mathrm{Re}(\lambda_i)$ changes sign, and therefore the equilibrium becomes locally unstable, when $T = 0$. With $H = \beta_2/(\beta_2 + \delta)$, we can write

$$T = \beta_1(2H^{1/q} - 1) - \frac{\beta_1 H^{1/q}(1 - H^{1/q})(\beta_1 + qH^{(q-1)/q})}{1 - H + \beta_1(1 - H^{1/q})}. \tag{A 3}$$

For $q = 4$ and $\beta_1 = 1/3$, one can symbolically solve $T = 0$ to obtain $H = c$, with $c = 0.2915$. This yields the equation for the bifurcation curve on the plane (β_2, δ):

$$\beta_2 = \frac{c}{1 - c}\delta, \tag{A 4}$$

which is a straight line with slope $c/(1 - c) = 0.4114$ and zero intercept. This is plotted in figure 4 for different values of β_2 and δ. One can also numerically show that the discriminant of the Jacobian matrix is negative, which implies that λ_i are a complex conjugate pair, on the entire (β_2, δ) plane. Thus, the approach to equilibrium is oscillatory.

REFERENCES

Abraham, E. R. 1998 The generation of plankton patchiness by turbulent stirring. *Nature* **391**, 577–580.

Alonso, D. & Solé, R. V. 2000 The Divgame simulator: a stochastic cellular automata model of rainforest dynamics. *Ecological Modelling* **133**, 131–141.

Bak, P., Tang, C. & Wiesenfeld, K. 1988 Self-organized criticality. *Phys. Rev.* A **38**, 364–374.

Bak, P., Chen, K. & Tang, C. 1990 A forest-fire model and some thoughts on turbulence. *Phys. Lett.* A **147**, 297–300.

Bennett, A. F. & Denman, K. L. 1985 Phytoplankton patchiness: inferences from particle statistics. *J. Mar. Res.* **43**, 307–335.

Blarer, A. & Doebeli, M. 1996 In the red zone. *Nature* **380**, 589–590.

Bradbury, R. H., Reichlet, R. E. & Green, D. G. 1984 Fractals in ecology: methods and interpretation. *Mar. Ecol. Prog. Ser.* **14**, 295–296.

Clar, S., Drossel, B., Schenk, K. & Schwabl, F. 1999 Self-organized criticality in forest-fire models. *Physica* A **266**, 153–159.

Clements, F. E. 1936 Nature and structure of the climax. *J. Ecol.* **24**, 252–284.

Cohen, J. E. 1995 Unexpected dominance of high frequencies in chaotic nonlinear population models. *Nature* **378**, 610–612.

Denman, K. L. & Platt, T. 1976 The variance spectrum of phytoplankton in a turbulent ocean. *J. Mar. Res.* **34**, 593–601.

Dewdney, A. K. 1988 *The armchair universe: an exploration of computer worlds*. New York: Freeman.

Dieckmann, U., Law, R. & Metz, J. A. J. 2000 *The geometry of ecological interactions. Simplifying spatial complexity*. Cambridge University Press.

Drossel, B. & Schwabl, F. 1992 Self-organized critical forest-fire model. *Phys. Rev. Lett.* **69**, 1629–1632.

Durrett, R. & Levin, S. 2000 Lessons on pattern formation from planet WATOR. *J. Theor. Biol.* **205**, 201–214.

Gabrielov, A., Newman, W. I. & Turcotte, D. L. 1999 An exactly soluble hierarchical clustering model: inverse cascades, self-similarity, and scaling. *Phys. Rev.* E **60**, 5293–5300.

Gleason, H. A. 1926 The individualistic concept of the plant association. *Bull. Torrey Bot. Club* **53**, 7–26.

Gower, J. F. R., Denman, K. L. & Holyer, R. J. 1980 Phytoplankton patchiness indicates the fluctuation spectrum of mesoscale oceanic structure. *Nature* **288**, 157–159.

Grassberger, P. 1993 On a self-organized critical forest-fire model. *J. Phys.* A **26**, 2081–2089.

Guichard, F., Allison, G., Halpin, P. & Levin, S.A. 2002 Mussel disturbance dynamics and the geometry of local interactions. *Am. Nat.* (Submitted.).

Hassell, M. P., Comins, H. N. & May, R. M. 1991 Spatial structure and chaos in insect population dynamics. *Nature* **353**, 255–258.

Hastings, H. M. & Sugihara, G. 1993 *Fractals: a user's guide for the natural sciences*. New York: Oxford University Press.

Hastings, H. M., Pekelney, R., Monticciolo, R., vun Kannon, D. & del Monte, D. 1982 Time scales, persistence, and patchiness. *Biosystems* **15**, 281–289.

Kaitala, V., Lundberg, P., Ripa, J. & Ylikarjula, J. 1997*a* Red, blue, green: dyeing population dynamics. *A. Zool. Fenn.* **34**, 217–228.

Kaitala, V., Ylikarjula, J., Ranta, E. & Lundberg, P. 1997*b* Population dynamics and the colour of environmental noise. *Proc. R. Soc. Lond.* B **264**, 943–994.

Keeling, M. 2000 Evolutionary dynamics in spatial host–parasite systems. In *The geometry of ecological interactions: simplifying spatial complexity* (ed. U. Diekmann, R. Law & A. J. Metz), pp. 271–289. Cambridge University Press.

Keitt, T. H. & Marquet, P. A. 1996 The introduced Hawaiian avifauna reconsidered: evidence for self-organized criticality. *J. Theor. Biol.* **182**, 161–167.

Keitt, T. H. & Stanley, H. E. 1998 Dynamics of North American breeding bird populations. *Nature* **393**, 257–260.

Korcak, J. 1938 Deux types fondamentaux de distribution statistique. *Bull. de l'Institut International de Statistique* **3**, 295–299.

Krummel, J. R., Gardner, R. H., Sugihara, G. & O'Neill, R. V. 1987 Landscape patterns in a disturbed environment. *Oikos* **48**, 321–384.

Levin, S. A. & Pacala, S. W. 1997 Theories of simplification and scaling of spatially distributed processes. In *Spatial ecology: the role of space in population dynamics and interspecific interactions* (ed. D. Tilman & P. Kareiva), pp. 271–296. Princeton University Press.

Malamud, B. D., Morein, G. & Turcotte, D. L. 1998 Forest fires: an example of self-organized critical behavior. *Science* **281**, 1840–1841.

Meltzer, M. I. & Hastings, H. M. 1992 The use of fractals to assess the ecological impact of increased cattle population: case study from the Runde Communal Land, Zimbabwe. *J. Appl. Ecol.* **29**, 635–646.

Miramontes, O. & Rohani, P. 1998 Intrinsically generated coloured noise in laboratory insect populations. *Proc. R. Soc. Lond.* B **265**, 785–792.

Morales, J. M. 1999 Viability in a pink environment: why 'white' noise models can be dangerous. *Ecol. Lett.* **2**, 228–232.

Nicholson, A. J. 1958 Dynamics of insect populations. *A. Rev. Entomol.* **3**, 107–136.

Pascual, M. & Levin, S. A. 1999 From individuals to population densities: searching for the intermediate scale of nontrivial determinism. *Ecology* **80**, 2225–2236.

Pascual, M., Mazzega, P. & Levin, S. A. 2001 Oscillatory dynamics and spatial scale: the role of noise and unresolved pattern. *Ecology* **82**, 2357–2369.

Petchey, O. L. 2000 Environmental colour affects aspects of single-species population dynamics. *Proc. R. Soc. Lond.* B **267**, 747–754.

Powell, T. M. & Okubo, A. 1994 Turbulence, diffusion and patchiness in the sea. *Phil. Trans. R. Soc. Lond.* B **343**, 11–18.

Rand, D. A. & Wilson, H. B. 1995 Using spatio-temporal chaos and intermediate-scale determinism to quantify spatially extended ecosystems. *Proc. R. Soc. Lond.* B **259**, 111–117.

Rand, D. A., Keeling, M. & Wilson, H. B. 1995 Invasion, stability and evolution to criticality in spatially extended artificial host–pathogen ecologies. *Proc. R. Soc. Lond.* B **259**, 55–63.

Rhodes, C. J. & Anderson, R. M. 1996 Power laws governing epidemics in isolated populations. *Nature* **381**, 600–602.

Rhodes, C. J., Jensen, H. J. & Anderson, R. M. 1997 On the critical behaviour of simple epidemics. *Proc. R. Soc. Lond.* B **264**, 1639–1646.

Smith, F. E. 1961 Density dependence in the Australian Thrips. *Ecology* **42**, 403–407.

Solé, R. V. & Manrubia, S. C. 1995 Self-similarity in rainforests: evidence for a critical state? *Phys. Rev.* E **51**, 6250–6253.

Sugihara, G. 1995 From out of the blue. *Nature* **378**, 559–560.

Sutherland, B. R. & Jacobs, A. E. 1994 Self-organization and scaling in a lattice predator–prey model. *Complex Systems* **8**, 385–405.

Weber, L. H., El-Sayed, S. Z. & Hampton, I. 1986 The variance spectra of phytoplankton, krill, and water temperature in the Antarctic Ocean south of Africa. *Deep-Sea Res.* **33**, 1327–1343.

Xiao-Ping, X., Qiong, G., Yi-Yin, L. & Zheng-Yu, Y. 1999 Fractal analysis of grass patches under grazing and flood disturbance in an alkaline grassland. *Acta Bot. Sinica* **41**, 307–313.

GLOSSARY

FFM: forest-fire model
SOC: self-organized criticality
2D: two dimensional
MDM: mussel-disturbance model